



## A BRIEF INTRODUCTION TO MATRIX HYDRODYNAMICS

KLAS MODIN<sup>✉\*1</sup> AND MILO VIVIANI<sup>✉2</sup>

<sup>1</sup>Mathematical Sciences, Chalmers and University of Gothenburg, Sweden

<sup>2</sup>Scuola Normale Superiore Pisa, Italy

*To the memory of Vladimir Zeitlin*

**ABSTRACT.** This survey gives a basic demonstration of matrix hydrodynamics; the field pioneered by V. Zeitlin, where 2-D incompressible fluids are spatially discretized via quantization theory.

**1. Introduction.** In October 2024, the mini-workshop “Geometric and Stochastic Methods for Fluid Models” was held at Kristineberg Station – one of the oldest marine biology stations in the world, situated in the western archipelago of Sweden. The participants, with varying backgrounds, were united in their zest for *matrix hydrodynamics*. This field began in the 1990s with the work of Vladimir Zeitlin, meteorologist and mathematician, who untimely passed away five months prior to the workshop. The survey is dedicated to his legacy.

In his breakthrough paper [36], Zeitlin used *quantization theory*, originally developed for applications in theoretical physics, as a numerical tool for spatial discretization of the 2-D Euler equations. This approach gives a finite-dimensional, isospectral matrix flow that captures the rich geometric structure of the 2-D Euler equations (Lie–Poisson structure, co-adjoint orbits, and Casimir functions, as surveyed below).

Zeitlin’s original method was developed for the flat torus and became known as the “sine-bracket approximation”. It initially gave rise to significant interest; the notion is so simple, beautiful, and different that it attracts attention. For example, McLachlan [25] found a Lie–Poisson preserving time integration scheme based on splitting. At large, however, numerical PDE analysts at the time concentrated on high-order methods. Zeitlin’s discretization has order  $1/2$ . Another criticism came from the fluid mechanics community. It was argued that numerical methods for 2-D Euler *should not* preserve enstrophy (one of the Casimirs), because enstrophy continuously disperse into smaller and smaller scales and this process cannot be resolved by any finite discretization. Finally, quantization on the flat torus has a problem: the translational symmetry is spoiled which implies Gibbs-like phenomenon. Later, Zeitlin [37] also derived his method for the sphere, on which the quantization preserves the rotational symmetry. But at the time it was unclear

2020 *Mathematics Subject Classification.* 35Q31, 53D50, 76M60, 76B47, 53D25.

*Key words and phrases.* Matrix hydrodynamics, two-dimensional turbulence, Euler equations, geometric hydrodynamics, quantization, Zeitlin’s model.

The authors would like to thank all the participants of the mini-workshop “Geometric and Stochastic Methods for Fluid Models”, Kristineberg, Sweden, October 2024.

\*Corresponding author: Klas Modin.

how the corresponding quantized Laplace–Beltrami operator could be efficiently inverted, which stood as a barrier for actual numerical simulations.

The abovementioned issues with Zeitlin’s method are justified. Yet, in the last couple of years, Zeitlin’s approach has seen a renaissance, with a rapidly growing number of activities, involving several groups with diverse backgrounds.

One reason is that focus now lies on the direct matrix formulation instead of truncated Fourier coordinates (as in the sine-bracket formulation). In turn, this setting enables highly optimized numerical linear algebra routines, such as threaded BLAS<sup>1</sup> algorithms for matrix-matrix multiplication. The emphasis on matrix formulations also warrants the name “matrix hydrodynamics”, as a general approach, using quantization theory to discretize hydrodynamic-like PDEs.

Another reason is the realization that high-order spatial discretizations are inessential for the 2-D Euler equations: individual trajectories generally diverge faster-than-exponential and are thus impossible to track for more than short time intervals, regardless of the order. To numerically study the long-time behavior, it is instead critical to preserve the underlying geometric structure of the equations. This point-of-view is strengthened by the physicists’ statistical mechanics approach to 2-D hydrodynamic. Indeed, as Onsager [33] first worked out, statistical mechanics predicts large-scale vortex condensation in the 2-D Euler equations, as observed in both experimental setups and real atmospheric flows (cf. [24, 5, 6]). Yet, statistical mechanics does not use the dynamics at all; it is entirely based on the geometric structure, namely the symplecticity of the phase flow and the conservation laws. Matrix hydrodynamics is thus a bridge between statistical mechanics and traditional numerical PDE methods based on locally tracking the dynamics (e.g., high-order Galerkin methods). A demonstration is provided by the statistically predicted Kraichnan spectrum for the inverse energy cascade in 2-D hydrodynamics [22], which is qualitatively captured with Zeitlin’s method, almost independently of the matrix size, but which traditional methods fail to capture even at significantly higher resolutions [9].

Finally, and perhaps most far-reaching, Zeitlin’s model and matrix hydrodynamics may *itself* give new mathematical tools for understanding the long-time behavior of 2-D hydrodynamics. An example is the *canonical scale separation* [31], which captures the inverse energy cascade and is based on tools from Lie group theory enabled via the matrix formulation. More generally, matrix hydrodynamics offer a way to distinguish finite-dimensional traits of the dynamics from those that are exclusively infinite-dimensional. For example, simulations with Zeitlin’s model show that the inverse energy cascade is structurally stable in this sense, if the underlying geometry is kept. As another example, preserving the Lie–Poisson geometry seems to produce a qualitatively correct distribution of enstrophy, albeit quantitatively exaggerated due to the finite dimensionality (cf. section 5 below), thus giving a new perspective on the criticism about conserving enstrophy.

This survey is a hands-on introduction to matrix hydrodynamics. As such, it requires little more than linear algebra and vector calculus. The focus is on Zeitlin’s model on the sphere, including a brief but complete illustration of how to carry out simulations with the Python code `quflow`. The wider, ongoing applications of matrix hydrodynamics are outlined, without details, in section 7. For a more in-depth introduction to matrix hydrodynamics, including quantization theory and numerical convergence, we refer to another publication of ours [32].

<sup>1</sup>See [netlib.org/blas/](https://netlib.org/blas/).

**2. Geometric hydrodynamics.** Let  $M$  be a Riemannian manifold comprising the vessel of an incompressible, inviscid fluid. Its motion is described by a time-dependent vector field  $\mathbf{v}(\mathbf{x}, t)$  on  $M$  fulfilling Euler's [15] equations

$$\dot{\mathbf{v}} + \nabla_{\mathbf{v}} \mathbf{v} = -\nabla p, \quad \operatorname{div} \mathbf{v} = 0, \quad (1)$$

where  $\dot{\mathbf{v}}$  denotes time derivative  $\frac{\partial \mathbf{v}}{\partial t}$ , the function  $p$  is the pressure, and  $\nabla_{\mathbf{v}}$  denotes the *co-variant derivative* in the direction of  $\mathbf{v}$  (i.e., the natural generalization of the directional derivative, from functions to vector fields).

Geometric hydrodynamics began with Arnold's [2] discovery that Euler's equations (1) describe geodesic motion on the group  $\operatorname{SDiff}(M)$  of volume preserving diffeomorphisms. The key is to think of  $\operatorname{SDiff}(M)$  as an infinite-dimensional Lie group. For  $\Phi \in \operatorname{SDiff}(M)$ , the tangent space  $T_{\Phi} \operatorname{SDiff}(M)$  then consists of maps of the form  $\mathbf{u} \circ \Phi$  where  $\mathbf{u}$  is a divergence free vector field on  $M$ . A Riemannian metric on  $\operatorname{SDiff}(M)$  is obtained by assigning to tangent vectors  $\mathbf{u} \circ \Phi$  and  $\mathbf{v} \circ \Phi$  the right-invariant  $L^2$  inner product

$$\langle \mathbf{u} \circ \Phi, \mathbf{v} \circ \Phi \rangle_{\Phi} = \int_M \mathbf{u} \cdot \mathbf{v}. \quad (2)$$

Arnold realized that if  $\mathbf{v}(x, t)$  is a solution to Euler's equations (1), then the corresponding curve of diffeomorphisms, obtained by solving the non-autonomous ordinary differential equation

$$\dot{\Phi} = \mathbf{v} \circ \Phi, \quad (\text{i.e., } \frac{\partial}{\partial t} \Phi(\mathbf{x}_0, t) = \mathbf{v}(\Phi(\mathbf{x}_0, t), t)),$$

is *geodesic* (locally length minimizing) for the metric (2). This Riemannian interpretation of incompressible hydrodynamics is more than a cute observation. It is a powerful tool that yields insights to the dynamics. For example, based on the geodesic formulation, Ebin and Marsden [12] gave improved existence and uniqueness results. Arnold himself made calculation of sectional curvatures, showing that it is mostly negative, which in turn has implication for the stability of fluids and for the non-existence of accurate long-time weather predictions [1, Appendix 2]. Many authors followed up on the curvature calculations, with further insights and results.

Geometric hydrodynamics provides a framework for studying the Euler equations (1), but is also, in its abstract form, applicable to a range of other equations (see Arnold and Khesin [3] and references therein). The general framework goes as follows. If  $G$  is a Lie group equipped with a right-invariant metric  $\langle \cdot, \cdot \rangle_g$  such that the length of a tangent vector  $\dot{g} = \xi g \in T_g G$  is

$$\langle \dot{g}, \dot{g} \rangle_g = \langle \dot{g} g^{-1}, \dot{g} g^{-1} \rangle_e = \langle \xi, \xi \rangle_e$$

then, in terms of the *momentum variable*  $\mu = \langle \xi, \cdot \rangle_e$ , the geodesic equation is

$$\dot{\mu} + \operatorname{ad}_{\xi}^* \mu = 0, \quad (3)$$

where  $\operatorname{ad}_{\xi}^*: \mathfrak{g}^* \rightarrow \mathfrak{g}^*$  is the infinitesimal adjoint action of the Lie algebra  $\mathfrak{g} = T_e G$  on its dual  $\mathfrak{g}^*$ . The equation (3) is the *Euler-Arnold equation* for the Lie algebra  $\mathfrak{g}$  equipped with the inner product  $\langle \cdot, \cdot \rangle_e$ .

Let us now derive these equations for the specific Lie algebra  $\mathfrak{g} = C_0^\infty(S^2)$  of smooth, zero-mean functions on the sphere equipped with the Poisson bracket

$$\{\psi, \xi\}(\mathbf{x}) = \mathbf{x} \cdot (\nabla \psi \times \nabla \xi) \quad (4)$$

for  $\mathbf{x} \in S^2 \subset \mathbb{R}^3$ . The Hamiltonian vector field corresponding to  $\psi$  is then given by the *skew-gradient*  $\nabla^\perp \psi = -\mathbf{x} \times \nabla \psi$ , as defined by  $\nabla^\perp \psi \cdot \nabla \xi = \{\xi, \psi\}$ .

As inner product on the Lie algebra, we take the Dirichlet energy

$$\langle \psi, \psi \rangle_e = \int_{S^2} |\nabla \psi|^2. \quad (5)$$

The corresponding momentum variable  $\omega = \langle \psi, \cdot \rangle_e$  is naturally, via the  $L^2$ -pairing, represented as the function  $\omega = -\Delta \psi$  for the Laplace-Beltrami operator  $\Delta$  on  $S^2$ . Indeed, from the divergence theorem

$$\langle \psi, \xi \rangle_e = \int_{S^2} \nabla \psi \cdot \nabla \xi = \int_{S^2} (-\operatorname{div} \nabla \psi) \xi = \int_{S^2} \underbrace{(-\Delta \psi)}_{\omega} \xi.$$

It remains to work out the adjoint action operator  $\operatorname{ad}_\psi^*$ . By definition,

$$\int_{S^2} (\operatorname{ad}_\psi^* \omega) \xi = \int_{S^2} \omega \{ \psi, \xi \}.$$

Standard vector calculus identities then yield

$$\begin{aligned} \int_{S^2} \omega \{ \psi, \xi \} &= \int_{S^2} \omega \nabla \xi \cdot (\mathbf{x} \times \nabla \psi) = - \int_{S^2} \xi \operatorname{div}(\omega \mathbf{x} \times \nabla \psi) = \\ &= - \int_{S^2} \xi \nabla \omega \cdot (\mathbf{x} \times \nabla \psi) = - \int_{S^2} \xi \{ \psi, \omega \}. \end{aligned}$$

Thus,  $\operatorname{ad}_\psi^* \omega = \{ \omega, \psi \}$ .<sup>2</sup> In summary, we have proved the following result.

**Proposition 2.1.** *The Euler–Arnold equation for the Lie algebra  $\mathfrak{g} = (C_0^\infty(S^2), \{ \cdot, \cdot \})$  equipped with the Dirichlet energy inner product (5) is*

$$\dot{\omega} + \{ \omega, \psi \} = 0, \quad -\Delta \psi = \omega. \quad (6)$$

Let us now work out the connection to the Euler equations (1). The curl (or skew-divergence) of a vector field  $\mathbf{v}$  on  $S^2$  is given by

$$\operatorname{curl} \mathbf{v} = \operatorname{div}(\mathbf{x} \times \mathbf{v}).$$

Applying this operator to the equations (1) yields

$$\operatorname{curl} \dot{\mathbf{v}} + \operatorname{curl} \nabla_{\mathbf{v}} \mathbf{v} = - \underbrace{\operatorname{curl} \nabla p}_{=0}.$$

Next,

$$\operatorname{curl} \nabla_{\mathbf{v}} \mathbf{v} = \mathbf{v} \cdot \nabla \operatorname{curl} \mathbf{v}$$

which we leave as an exercise to prove. Consequently,

$$\operatorname{curl} \dot{\mathbf{v}} + \mathbf{v} \cdot \nabla \operatorname{curl} \mathbf{v} = 0,$$

so  $\operatorname{curl} \mathbf{v}$  is advected by the vector field  $\mathbf{v}$ .

Since the vector field  $\mathbf{v}$  is divergence free, and thus symplectic with respect to the area-form, and since the first co-homology of the sphere is trivial, we obtain that  $\mathbf{v} = \nabla^\perp \psi$  for some Hamiltonian  $\psi$  which is unique up to a constant (in particular, it is unique in  $C_0^\infty(S^2)$ ). Since  $\operatorname{curl} \nabla^\perp \psi = \operatorname{div}(\mathbf{x} \times (-\mathbf{x} \times \nabla \psi)) = -\Delta \psi$  and since  $\{ \omega, \psi \} = \nabla^\perp \psi \cdot \nabla \omega$ , we obtain that  $\omega = \operatorname{curl} \mathbf{v}$  fulfills the Euler–Arnold equation (6). This is, of course, the vorticity formulation of the 2-D Euler equations. In summary, we have the following result.

<sup>2</sup>The calculation also shows that the  $L^2$  inner product is *bi-invariant*, namely  $\langle \omega, \{ \psi, \xi \} \rangle_{L^2} = \langle -\{ \psi, \omega \}, \xi \rangle_{L^2}$ , which means that  $L^2$  is canonical with respect to the Lie algebra structure. In particular, the geodesics generated by this inner product coincides with the group exponential.

**Corollary 2.2.** *The Euler equations (1) on the domain  $M = S^2$  are equivalent to the Euler–Arnold equation (6). The vorticity function, corresponding to the momentum variable, is given by  $\omega = \text{curl } \mathbf{v}$ , whereas the stream function  $\psi$  is the Hamiltonian for the vector field, so that  $\mathbf{v} = \nabla^\perp \psi$ .*

**3. The Euler–Zeitlin equations.** Zeitlin [36] had the brilliant idea to use quantization theory for spatial discretization of the vorticity form (6) of the 2-D Euler equations. The aim of quantization theory is to find a mapping between smooth functions and Hermitian linear operators on a Hilbert space such that the Poisson bracket between functions corresponds, up to scaling by  $i/\hbar$ , to the commutator between operators. If the underlying domain is compact, then the Hilbert space can be finite-dimensional, so the operators are Hermitian matrices. In the context of matrix hydrodynamics, we work with skew-Hermitian matrices  $\mathfrak{u}(N)$  instead (multiplication by the imaginary unit  $i$  provides an isomorphism).

For the Poisson bracket (4) on the sphere, we thus seek a linear mapping

$$C^\infty(S^2) \ni \psi \mapsto T_N \psi \in \mathfrak{u}(N)$$

such that the image of the Poisson bracket  $T_N\{\psi, \omega\}$  is approximated by the scaled commutator  $\frac{1}{\hbar}[T_N \psi, T_N \omega]$  for  $\hbar = 2/\sqrt{N^2 - 1}$ . Of course, this is trivially achieved by taking  $T_N \equiv 0$ , so we also require a consistency condition, typically  $T_N 1 = -iI$  (the constant function 1 is mapped to  $-i$  times the identity matrix) and  $\|T_N^* T_N \psi - \psi\|_{L^2} \rightarrow 0$  as  $N \rightarrow \infty$ , where  $T_N^*: \mathfrak{u}(N) \rightarrow C^\infty(S^2)$  denotes the  $L^2$  adjoint of  $T_N$ . Such a quantization was given by Berezin [4] and by Hoppe [20]. More generally, *Berezin–Toeplitz quantization* is applicable to any quantizable symplectic manifold (see the monograph by Le Floch [23] for details). Sharp convergence results were given by Charles and Polterovich [7].

For the sphere, quantization is best understood via representation theory. Indeed, from a unitary  $\mathfrak{so}(3)$  representation, generated by  $S_1, S_2, S_3 \in \mathfrak{u}(N)$ , we obtain the *Casimir operator*.

$$\Delta_N: \mathfrak{u}(N) \rightarrow \mathfrak{su}(N), \quad \Delta_N P = \sum_{\alpha=1}^3 [S_\alpha, [S_\alpha, P]]. \quad (7)$$

As pointed out by Hoppe and Yau [21], this operator gives an approximation of the Laplace–Beltrami operator on  $S^2$ , with the same spectrum up to truncation at the maximum spherical harmonics wave-number  $\ell = N - 1$ . For details on the representation point-of-view of quantization, see Modin and Viviani [32, sect. 3].

We now have all the ingredients to approximate the 2-D Euler equations (6) via quantization theory. Indeed, the *Euler–Zeitlin equations* is the isospectral flow of matrices on  $\mathfrak{su}(N)$  given by

$$\dot{W} + \frac{1}{\hbar}[W, P] = 0, \quad -\Delta_N P = W, \quad (8)$$

where  $\hbar = 2/\sqrt{N^2 - 1}$ . The isospectral property of the flow (8) reflects the advection property of the vorticity equation (6). It implies conservation of *Casimirs functions*

$$C_f^N(W) = \frac{4\pi}{N} \text{tr}(f(iW)),$$

for any smooth function  $f: \mathbb{R} \rightarrow \mathbb{R}$ . These converge to the corresponding continuous Casimirs  $C_f(\omega) = \int_{S^2} f(\omega)$  as  $N \rightarrow \infty$  [32]. However, the key-point of matrix hydrodynamics is *not* conservation of Casimirs. Rather, the conservation laws is

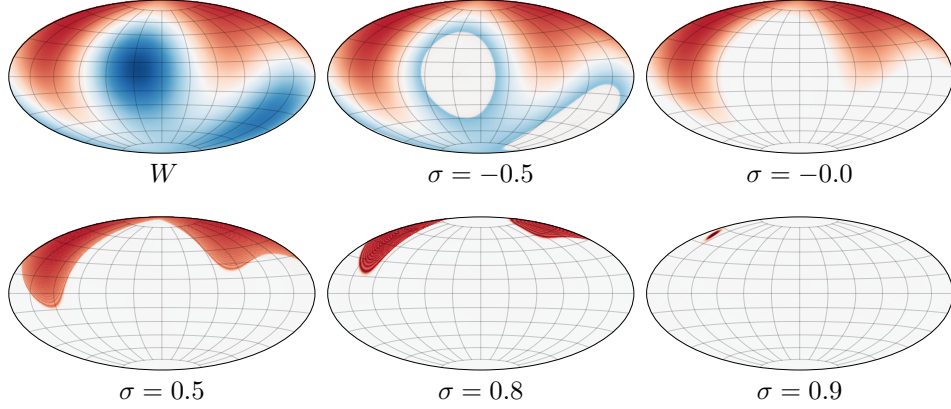


FIGURE 1. A skew-Hermitian matrix  $W \in \mathfrak{su}(512)$ , with eigenvalues  $-i\lambda_1, \dots, -i\lambda_{512}$  such that  $-1 \leq \lambda_m \leq 1$  and corresponding eigenvectors  $\mathbf{e}_m$ , is partially reconstructed by  $\sum_{i\lambda_m \geq \sigma} -i\lambda_m \mathbf{e}_m \mathbf{e}_m^\dagger$  for  $\sigma \in [-1, 1]$ . As seen in the figure, this decomposition corresponds to nullifying the level-sets of the vorticity function with values below  $\sigma$ . The sphere is visualized via the area-preserving Hammer projection.

a consequence of a deeper analog: just as the level-sets of the continuous vorticity field  $\omega$  are advected, the eigenvectors  $\mathbf{e}_i$  of the vorticity matrix  $W$  are ‘advected’ as

$$\dot{\mathbf{e}}_i = \frac{1}{\hbar} P \mathbf{e}_i, \quad (9)$$

while the corresponding eigenvalues  $-i\lambda_i$  of  $W$  are preserved.<sup>3</sup> This is readily seen since  $W = \sum_{k=1}^N -i\lambda_k \mathbf{e}_k \mathbf{e}_k^\dagger$  so the discrete advection equations (9) yield

$$\dot{W} = \sum_{k=1}^N \frac{-i\lambda_k}{\hbar} (\mathbf{e}_k (P \mathbf{e}_k)^\dagger + (P \mathbf{e}_k) \mathbf{e}_k^\dagger) = -\frac{1}{\hbar} [W, P].$$

See Figure 1 for an illustration of the correspondences

level-sets  $\leftrightarrow$  eigenvectors      and      vorticity values  $\leftrightarrow$  eigenvalues.

These correspondences are at the heart of matrix hydrodynamics. They enable numerical studies of the *structural stability* of the 2-D Euler equations (6). Namely, to study if long-time, qualitative properties of its solutions are stable under perturbations of the underlying infinite-dimensional Lie-Poisson structure (to the finite-dimensional Lie-Poisson structure underlying the Euler–Zeitlin equations).

**3.1. The isospectral midpoint method.** To simulate the Euler–Zeitlin equations (8) we need a suitable time integration method. Ideally, to be useful for structural stability studies, the method should preserve the finite-dimensional Lie–Poisson structure of the Euler–Zeitlin equations. In particular, it should preserve

<sup>3</sup>These equations allow for a ‘transport formulation’ of the Euler–Zeitlin equations, which can be used as a basis for time-discretization, as explored in the paper ? of this special issue.

the isospectral property of the flow.<sup>4</sup> Such an integration scheme is given by the *isospectral midpoint method* [30], which is the mapping  $W_n \mapsto W_{n+1}$  defined via an intermediate stage  $\tilde{W}$  by

$$\begin{aligned} W_n &= \tilde{W} - \frac{\varepsilon}{2}[\tilde{W}, \tilde{P}] - \frac{\varepsilon^2}{4}\tilde{P}\tilde{W}\tilde{P}, \\ \Delta_N \tilde{P} &= \tilde{W} \\ W_{n+1} &= W_n - \varepsilon[\tilde{W}, \tilde{P}], \end{aligned} \tag{10}$$

where  $\varepsilon = \delta t/\hbar$  for a chosen time-step  $\delta t$ . An efficient implementation of the scheme (10) is given by Cifani, Viviani, and Modin [10].

In addition to preserving the Lie–Poisson structure, the isospectral midpoint method is reversible with respect to  $P \mapsto -P$ . Further, it is second order accurate in time.<sup>5</sup>

**4. A numerical illustration.** In this section, we demonstrate the Python package `quflow`<sup>6</sup> for simulating the 2-D Euler equations (6) via the Euler–Zeitlin equations (8) discretized in time by the isospectral midpoint method (10). The first step is to load the package and specify the initial vorticity field by spherical harmonics coefficients.

```
import numpy as np
import quflow as qf

# Initial conditions as random real spherical harmonics
# truncated at wave-number 'elmax'
elmax = 20
omega0 = np.random.randn((elmax+1)**2)

# Set vanishing mean
omega0[0] = 0.0

# Set vanishing total angular momentum
omega0[1:4] = 0.0

# Create corresponding initial matrix with size 'N'
N = 512
W0 = qf.shr2mat(omega0, N)

# Plot the initial vorticity field
qf.plot(omega0, colorbar=True)
```

The call to `qf.plot` displays the initial vorticity field, as seen in Figure 2.

<sup>4</sup>Notice, however, that preserving the Lie–Poisson structure is a much stronger condition than preserving isospectrality. Geometrically, isospectrality means that the motion remains on a single *co-adjoint orbit*, whereas Lie–Poisson means that the flow is symplectic on that orbit.

<sup>5</sup>It is impossible to accurately track exact solutions for more than short time intervals, regardless of the order of the method. However, higher order methods may still be useful, for example to more accurately conserve energy or in the study of stationary solutions. [cross citation to special issue paper by da Silva, Viviani, and Lessig]

<sup>6</sup>Available at [github.com/klasmodin/quflow/](https://github.com/klasmodin/quflow/). It is installed via the pip package manager.



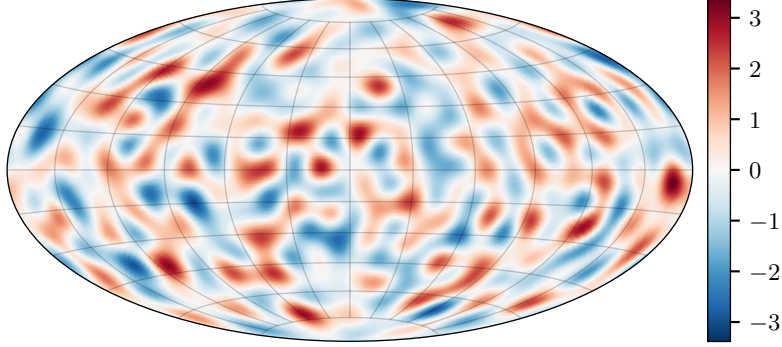


FIGURE 2. Initial vorticity field, generated as a truncated spherical harmonic series  $\sum_{\ell=0}^{\ell_{\max}} \sum_{m=-\ell}^{\ell} \omega_{\ell,m} Y_{\ell,m}$  where  $\ell_{\max} = 20$  and the coefficients  $\omega_{\ell,m}$  are normally distributed.

Next, the output data file is initialized, and the solver parameters are specified.

```
# Create simulation data file
sim = qf.QuSimulation("quflow_sim.hdf5", state=W0, overwrite=True)

# Set simulation parameters
sim['dt'] = 0.2*qf.hbar(N)
sim['simtime'] = 100.0
sim['dt_out'] = 0.2
```

Notice that we have specified the time step length  $\Delta t$  in units of  $\hbar$ . This way, the time step scales correctly when we change the matrix size  $N$ .

The final step is to run the simulation, i.e., to carry out time integration via the isospectral midpoint method (10).

```
# Run the simulation
qf.solve(sim)
```

Once the simulation is finished, the results are stored in the hdf5 file format. The default setting stores both function values on a grid in spherical coordinates (in the hdf5-field `'fun'`) and the corresponding  $\mathfrak{su}(N)$  matrices (in the hdf5-field `'mat'`). For example, the following code displays the last output and extracts the corresponding matrix.

```
# Load simulation results
sim = qf.QuSimulation("quflow_sim.hdf5")

# Plot the last output
qf.plot(sim['fun'], -1)

# Extract matrix of the last output
W = sim['mat', -1]
```



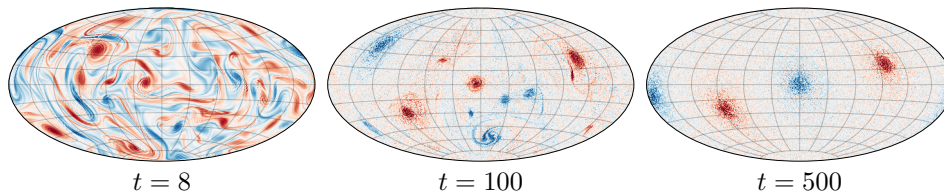


FIGURE 3. Evolution of the vorticity field for the `quflow` simulation in Section 4, with initial data as in Figure 2. Vorticity regions of equal sign undergo mixing until four “vortex blob-condensates” remain, two positive and two negative. After that, the large-scale motion stabilizes in quasi-periodic interaction between the blobs.

Snapshots of the simulated vorticity evolution are given in Figure 3. The initial vorticity field undergoes intricate mixing, where nearby vorticity regions of equal sign continue to merge until only a few “vortex blobs” remain. Typically, the merging stops at 4 blobs if the total angular momentum is zero, corresponding to the integrable motion of 4 point vortices with vanishing angular momentum, and at 3 blobs for non-vanishing total angular momentum, corresponding to integrable motion of 3 point vortices. More details on this mechanism, as well as further numerical experiments, are given by the authors in a prior publication [29].

**5. Conservation of enstrophy implies noise.** Consider the expansion of vorticity in spherical harmonics

$$\omega = \sum_{\ell=1}^{\infty} \sum_{m=-\ell}^{\ell} \omega_{\ell,m} Y^{\ell,m},$$

where  $\ell$  corresponds to the wave-number frequency ( $V^{\ell} = \text{span}(Y^{\ell,-\ell}, \dots, Y^{\ell,\ell})$  is the eigenspace of the Laplace-Beltrami operator with eigenvalue  $-\ell(\ell+1)$ ). The long-time behavior of the 2-D Euler equations can be addressed by studying the statistical properties of the coefficients  $\omega_{\ell,m}$ . Indeed, for low wave-numbers, say  $\ell < \ell^*$ , we expect a build-up of energy (cf. *inverse energy cascade*), whereas for high wave-numbers,  $\ell > \ell^*$ , we expect as  $t \rightarrow \infty$  a uniform distribution of the spherical harmonics coefficients (cf. *forward enstrophy cascade*). Thus, for  $\ell > \ell^*$  we expect, in average, that  $\omega_{\ell,m}^2 \sim \varepsilon^2$  with an infinitesimal noise-level  $\varepsilon^2$  as  $t \rightarrow \infty$ . Details of the underlying theoretical models, as well as numerical and experimental verification, are covered in the survey by Boffetta and Ecke [5].

As we have seen, the long-time simulations based on the Euler-Zeitlin equations (8) typically settle at a few interacting vortex blobs for the large-scale dynamics. On small scales, however, there is a background “noise”, moderate but significant in magnitude. This noise is qualitatively correct, but quantitatively incorrect: its magnitude is exaggerated.

The magnification of the background noise is a consequence of conservation of enstrophy, i.e., conservation of the Casimir

$$C_2 = \int_{S^2} \omega^2 = \sum_{\ell=1}^{\infty} \sum_{m=-\ell}^{\ell} \omega_{\ell,m}^2.$$

Indeed, for the Zeitlin model we have

$$W = \sum_{\ell=1}^{N-1} \sum_{m=-\ell}^{\ell} \omega_{\ell,m}^N T_N^{\ell,m},$$

where  $T_N^{\ell,m}$  are the eigenmatrices of the Hoppe–Yau Laplacian  $\Delta_N$  directly corresponding to the spherical harmonics  $Y^{\ell,m}$ . By introducing  $(\omega_\ell^N)^2 = \sum_{m=-\ell}^{\ell} \omega_{\ell,m}^N$ , and under the assumption  $N > \ell^*$  we decompose the enstrophy as

$$C_2 = \sum_{\ell=1}^{\ell^*-1} (\omega_\ell^N)^2 + \underbrace{\sum_{\ell=\ell^*}^{N-1} (\omega_\ell^N)^2}_a.$$

In the long-time states, the large-scale blobs are accounted for in the first part of the sum. It is natural to assume that this large-scale part is mostly unaffected by  $N$ , as long as  $N$  is large enough in comparison to  $\ell^*$  (e.g., at least twice as large). Consequently, since enstrophy is conserved,  $a$  is an adiabatic invariant largely independent of  $N$ . If we furthermore assume that the Zeitlin model produces the qualitatively correct statistics, so that the small-scale states  $(\omega_{\ell,m}^N)^2$  independently average to  $\varepsilon^2$ , we get that  $(\omega_\ell^N)^2 \approx (2\ell + 1)\varepsilon^2$ . These assumptions allow us to express  $\varepsilon^2$  in terms of  $a$  and  $N$ :

$$a = \sum_{\ell=\ell^*}^{N-1} (\omega_\ell^N)^2 \approx \varepsilon^2 \sum_{\ell=\ell^*}^{N-1} (2\ell + 1) \iff \varepsilon^2 \approx \frac{a}{\sum_{\ell=\ell^*}^{N-1} (2\ell + 1)}.$$

In particular, we expect that the noise-level  $\varepsilon^2$  decreases as  $\mathcal{O}(N^{-2})$  as  $N \rightarrow \infty$  whereas  $a$  remains largely independent of  $N$ . Figure 4 confirms this behavior.

That enstrophy conservation in a numerical method for the 2-D Euler equations imply excessive background noise is an argument against conservation of enstrophy (and more specifically against conservation of co-adjoint orbits). Indeed, it is common to introduce “numerical viscosity” to model the dispersion of enstrophy into small scales (see, e.g., the study by Dritschel, Qi, and Marston [11]). However, the mechanism of enstrophy dispersion (forward cascade and mixing) in the 2-D Euler equations is distinct from the mechanism of viscosity or other types of damping. Indeed, numerical viscosity tend to destroy the theoretically predicted properties of the long-time behavior, as such behavior often hinges on the advection of vorticity and thus on the conservation of co-adjoint orbits. For example, the theoretically predicted Kraichnan spectrum for forced 2-D turbulence is captured in the Zeitlin model, chiefly independently of  $N$ , whereas traditional methods (with numerical viscosity) fail to capture it even at significantly higher resolutions [9]. In our experience, for numerical studies of the long-time behavior, a viable strategy is to use Zeitlin-based discretizations and then carefully taking the background noise into account for the conclusions (the noise can be estimated via the model above). This allows for simulations that capture the long-time behavior contingent on vorticity advection as long as that behavior is stable under amplified background noise.

**5.1. Hyperviscosity to reduce the noise.** There could be situations where the noise induced by conservation of enstrophy is undesirable. For example, to compare the results of a structure preserving simulation with one where enstrophy dissipates. In such situations, one can introduce *hyperviscosity* to the Euler–Zeitlin

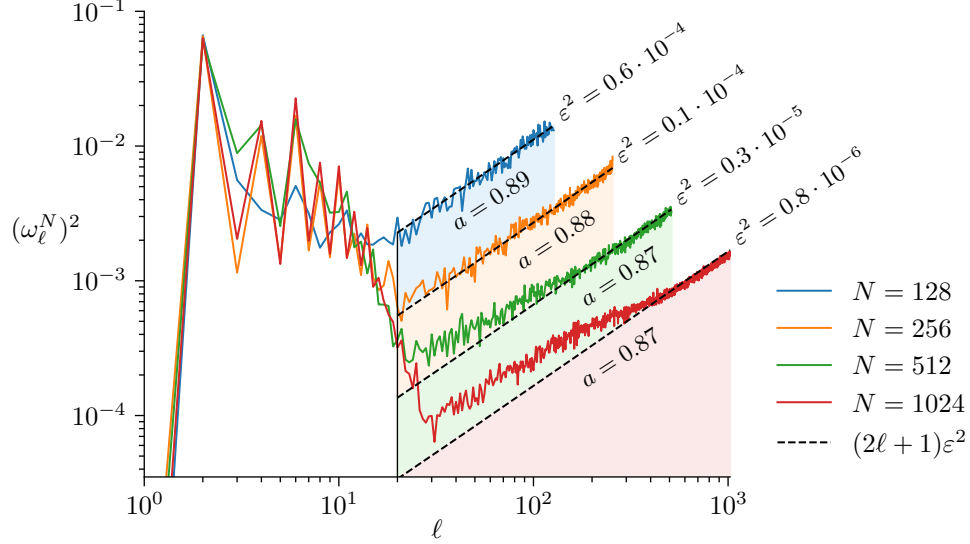


FIGURE 4. Visualization of the long-time spectral enstrophy components  $(\omega_\ell^N)^2 = \sum_{m=-\ell}^{\ell} (\omega_{\ell,m}^N)^2$  for varying matrix sizes  $N$ . The initial data is the same as in Figure 2. On small enough scales,  $\ell > \ell^* \approx 20$ , enstrophy gets uniformly distributed among the spherical harmonics coefficients  $(\omega_{\ell,m}^N)^2$ , such that  $(\omega_\ell^N)^2 \approx (2\ell + 1)\varepsilon^2$ . For a smaller  $N$ , there is “less room” in phase space to distribute enstrophy, resulting in a larger background noise  $\varepsilon^2$ . That the areas  $a$  under the graphs are largely independent of  $N$  verifies this discussion.

equations (8), namely

$$\dot{W} + \frac{1}{\hbar}[W, P] = \frac{\nu}{\hbar^2}[P, [P, W]], \quad -\Delta_N P = W, \quad (11)$$

where  $\nu \geq 0$  is the hyperviscosity parameter (usually small). The force is dissipative, similar to viscosity in the Navier–Stokes equations, except that it is non-linear and preserves the energy.

**Proposition 5.1.** *The energy (i.e., the Hamiltonian for the Euler–Zeitlin equations)*

$$H = \frac{2\pi}{N} \operatorname{tr}(W^\dagger P)$$

*is conserved by the hyperviscous Euler–Zeitlin equations (11).*

*Proof.* Direct calculations give

$$\begin{aligned} \frac{d}{dt} \frac{2\pi}{N} \operatorname{tr}(PW) &= \frac{4\pi}{N} \operatorname{tr} \left( P \left( \frac{1}{\hbar}[P, W] + \frac{\nu}{\hbar^2}[P, [P, W]] \right) \right) = \\ &= \frac{4\pi\nu}{N\hbar^2} \operatorname{tr} \left( -\underbrace{[P, P]}_0 [P, W] \right) = 0. \end{aligned}$$

□

On the other hand, hyperviscosity dissipates convex Casimirs.

**Proposition 5.2.** *Let  $f: \mathbb{R} \rightarrow \mathbb{R}$  be a convex function. Then the corresponding Casimir*

$$C_f^N(W) = \frac{4\pi}{N} \operatorname{tr}(f(iW))$$

*decays along solutions of the hyperviscous Euler–Zeitlin equations (11).*

To prove this result, we need the following result.

**Lemma 5.3.** *Let  $W, W' \in \mathfrak{u}(N)$  with  $[W, W'] = 0$  and denote by  $iw_1, \dots, iw_N$  and  $iw'_1, \dots, iw'_N$  their eigenvalues, ordered with respect to a common eigenbasis  $F \in U(N)$ . Then, for any  $X \in \mathfrak{u}(N)$ ,*

$$\operatorname{tr}([X, W]^\dagger [X, W']) = \sum_{m=-N}^N \sum_{i=1}^{n-|m|} |Y_{m \setminus i}|^2 (w'_{i+|m|} - w'_i)(w_{i+|m|} - w_i),$$

where  $Y = F^\dagger X F$  and  $Y_{m \setminus i}$  denotes the  $i$ :th element along the  $m$ :th diagonal of  $Y$ .

*Proof.* Since  $[W, W'] = 0$  we can find a common eigenbasis  $F \in U(n)$  which diagonalizes them. Then

$$\operatorname{tr}([X, W]^\dagger [X, W']) = \operatorname{tr}([Y, D_W]^\dagger [Y, D_{W'}])$$

where  $Y = F^\dagger X F$ ,  $D_W = i \operatorname{diag}(w_1, \dots, w_n)$ , and  $D_{W'} = i \operatorname{diag}(w'_1, \dots, w'_n)$ . Via a direct calculation

$$\operatorname{tr}([Y, D_W]^\dagger [Y, D_{W'}]) = \sum_{m=-N}^N \sum_{i=1}^{N-|m|} |Y_{m \setminus i}|^2 (p_{i+|m|} - p_i)(w_{i+|m|} - w_i).$$

□

*Proof of Proposition 5.2.* Along the flow of (11) we have

$$\begin{aligned} \frac{d}{dt} C_f^N &= \frac{d}{dt} \frac{4\pi}{N} \operatorname{tr}(f(iW)) = \frac{4\pi i}{N} \operatorname{tr} \left( f'(iW) \left( \frac{1}{\hbar} [P, W] + \frac{\nu}{\hbar^2} [P, [P, W]] \right) \right) = \\ &= -\frac{4\pi \nu i}{N \hbar^2} \operatorname{tr}([P, f'(iW)][P, W]) = \\ &= -\frac{4\pi \nu}{N \hbar^2} \sum_{m=-N}^N \sum_{i=1}^{n-|m|} |Y_{m \setminus i}|^2 (f'(w_{i+|m|}) - f'(w_i))(w_{i+|m|} - w_i), \end{aligned}$$

where the last equality follows from Lemma 5.3 for  $Y = F^\dagger P F$ . Then, from the mean value theorem, we obtain

$$\begin{aligned} &= -\frac{4\pi \nu}{N \hbar^2} \sum_{m=-N}^N \sum_{i=1}^{n-|m|} |Y_{m \setminus i}|^2 (f'(w_{i+|m|}) - f'(w_i))(w_{i+|m|} - w_i) = \\ &= -\frac{4\pi \nu}{N \hbar^2} \sum_{m=-N}^N \sum_{i=1}^{n-|m|} |Y_{m \setminus i}|^2 f''(\xi_{im})(w_{i+|m|} - w_i)^2 \end{aligned}$$

for  $\xi_{im} \in [w_i, w_{i+|m|}]$ . Since  $f$  is convex,  $f'' \geq 0$  which proves the result. □

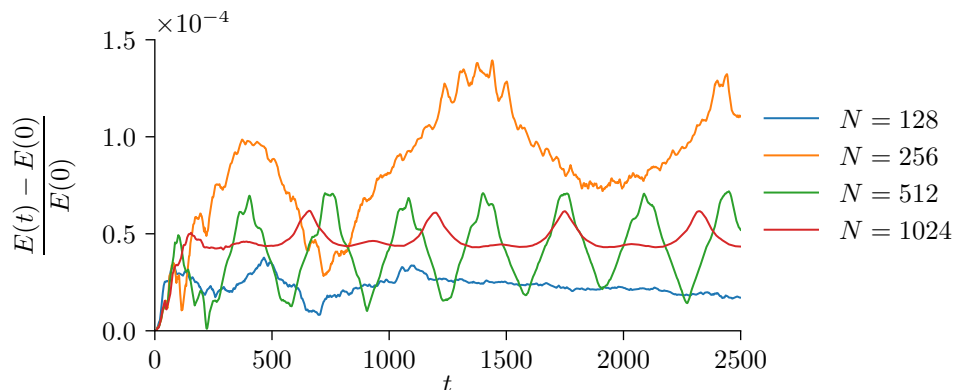


FIGURE 5. Evolution of the relative energy error for varying matrix sizes  $N$ . The initial data is the same as in Figure 2. Notice that the energy is “nearly conserved” in the sense compatible with the backward error analysis for symplectic integrators. There is no indication that the errors grow with  $N$ . We currently lack a rigorous analysis of this behavior, since backward error analysis, as developed for finite-dimensional Hamiltonian systems, prevents control over  $N$ .

**6. Near conservation of energy.** The isospectral midpoint method (10) exactly conserves Casimirs for the Euler–Zeitlin equations (8). But it fails to exactly conserve energy. One can view this as a consequence of the method being symplectic on the co-adjoint orbits: a method exactly conserving energy and symplecticity for a non-integrable system implies exact tracking of trajectories up to time-reparameterization [40]. Yet, since the co-adjoint orbits for  $\mathfrak{su}(N)$  are compact for a fixed  $N$ , we can expect that energy is “nearly conserved” in the sense of backward error analysis (BEA) for symplectic integrators (cf. Hairer, Lubich, and Wanner [19] and references therein). But there is a problem with this argument: we are interested in the behavior for large  $N$  whereas there is no control on how the estimates in BEA depend on  $N$ . Therefore, BEA, as developed for finite-dimensional Hamiltonian system, cannot rigorously be used to address near conservation of energy in simulations based on the Euler–Zeitlin equations. Numerical experiments nevertheless suggest that energy is nearly preserved independently of  $N$ , as illustrated in Figure 5.

**Open Problem.** Develop backward error analysis (for the isospectral midpoint method applied to the Euler–Zeitlin equations) that rigorously explains the numerically observed near conservation of energy.

**7. Further topics.** In this survey, we focus on the Euler–Zeitlin equations (8) as an approximation to the 2-D Euler equations on the sphere. But this setting is only the beginning of matrix hydrodynamics; the approach can be used for many other equations. The general principle is to use quantization theory to replace functions by matrices and the Poisson bracket with the (scaled) commutator. Below we exemplify recent developments.

**7.1. Geophysical fluid dynamics.** Two-dimensional models naturally appear in geophysical fluid dynamics, via the quasi-geostrophic equation and its variants (cf. [39]). A matrix hydrodynamics version of the global quasi-geostrophic equation is given by Franken, Caliaro, Cifani, and Geurts [16], where the authors provide simulations that qualitatively captures the turbulent band structures observed in the atmosphere of Jupiter. Based on this work, further analysis of the critical latitude for jet formation is provided by the same authors [17].

The underlying Riemannian geometric structure of the global quasi-geostrophic equations is specified by Modin and Suri [28]. This structure enables stability analysis based on sectional curvature calculations. In particular, the study shows that the *Lamb parameter* in the global quasi-geostrophic model has a stabilizing effect on the dynamics.

The matrix hydrodynamics approach has also been extended to multi-layer quasi-geostrophic models on the sphere [18]. The resulting method enables long-term simulations without additional regularization, and the study highlights the importance of structure-preserving techniques for understanding large-scale geophysical flows.

Roop and Ephrati [35] also derive a global model of thermal quasi-geostrophy on the sphere, based on the thermal rotating shallow water equations, and give a corresponding matrix hydrodynamics discretization. Simulations with this method reveal the formation of vorticity and buoyancy fronts, and large-scale structures in the buoyancy dynamics induced by the buoyancy-bathymetry interaction.

**7.2. Reduced magnetohydrodynamics.** Reduced magnetohydrodynamics constitute a two-dimensional system of PDEs and constitute a simple model for both astrophysical and laboratory plasmas. A matrix hydrodynamics model for this system, in the case of the flat torus, is given by Zeitlin [38]. Contrary to the Euler–Zeitlin equations, the matrix flow is only partially isospectral. An analogous model on the sphere, together with an extension of the spherical midpoint method to the underlying semi-direct Lie algebra, is given by Modin and Roop [27].

**7.3. Stochastic hydrodynamics.** The Euler–Zeitlin equations and the isospectral midpoint method can be extended to stochastic versions, via the addition of *transport noise*, as developed by Ephrati, Jansson, Lang, and Luesink [14]. The authors prove almost sure preservation of Casimir functions and coadjoint orbits under the numerical flow and provide strong and weak convergence rates of the proposed method.

**7.4. Model reduction techniques.** The isospectral matrix flow formulations in matrix hydrodynamics allow for model reduction, based, for example, on the matrix eigenspaces. Such considerations are given by Ephrati, Cifani, Viviani, and Geurts [8, 13], and by Pagliantini [34]. This approach has the potential to significantly reduce the complexity of the Euler–Zeitlin equations and the isospectral midpoint methods, from  $\mathcal{O}(N^3)$  to  $\mathcal{O}(N^2)$ , thus on par with the complexity of conventional methods such as finite elements, but retaining the structural benefits of matrix hydrodynamics.

**7.5. Axisymmetric three-dimensional Euler equations.** All the developments listed so far has been on two-dimensional domains (typically the sphere). Indeed, the matrix hydrodynamics approach fail to directly extend to three-dimensional domains. Essentially, this limitation stems from quantization, which relies on the

symplectic structure of two-dimensional, compact manifolds, and the fact that incompressibility then implies that the fluid velocity field is Hamiltonian. Nevertheless, the *axisymmetric* 3-D Euler equations on the 3-sphere admits a matrix hydrodynamics discretization, as developed by Modin and Preston [26]. Numerical simulations based on this method shows a faster-than-exponential growth of the maximum vorticity. The authors also use the finite-dimensional model to study Riemannian curvature and Jacobi equations in the context of axisymmetric 3-D Euler.

**Acknowledgments.** This work was supported by the Swedish Research Council (grant number 2022-03453), the Knut and Alice Wallenberg Foundation (grant numbers WAF2019.0201), and the Göran Gustafsson Foundation for Research in Natural Sciences and Medicine. The computations were enabled through resources provided by Chalmers e-Commons at Chalmers and by the National Academic Infrastructure for Supercomputing in Sweden (NAISS), partially funded by the Swedish Research Council through grant no. 2022-06725. Finally, the authors thank SVEFUM for funding the workshop “Geometric and Stochastic Methods for Fluid Models”, which eventually led to the special issue at hand.

## REFERENCES

- [1] V. I. Arnold. *Mathematical Methods of Classical Mechanics*, volume 60 of *Graduate Texts in Mathematics*. Springer-Verlag, New York, second edition, 1989.
- [2] Vladimir Arnold. Sur la géométrie différentielle des groupes de Lie de dimension infinie et ses applications à l’hydrodynamique des fluides parfaits. *Ann. Inst. Fourier (Grenoble)*, 16:319–361, 1966.
- [3] Vladimir Arnold and Boris Khesin. *Topological methods in hydrodynamics*, volume 125 of *Applied Mathematical Sciences*. Springer, Cham, Second edition, 2021.
- [4] F. A. Berezin. General concept of quantization. *Comm. Math. Phys.*, 40:153–174, 1975.
- [5] G. Boffetta and R. E. Ecke. Two-dimensional turbulence. *Ann. Rev. Fluid Mech.*, 44(1):427–451, 2012.
- [6] Freddy Bouchet and Antoine Venaille. Statistical mechanics of two-dimensional and geophysical flows. *Physics reports*, 515(5):227–295, 2012.
- [7] L. Charles and L. Polterovich. Sharp correspondence principle and quantum measurements. *St. Petersburg Math. J.*, 29(1):177–207, 2018.
- [8] P. Cifani, S. Ephrati, and M. Viviani. Sparse-stochastic model reduction for 2d euler equations, 2023.
- [9] P. Cifani, M. Viviani, E. Luesink, K. Modin, and B. Geurts. Casimir preserving spectrum of two-dimensional turbulence. *Phys. Rev. Fluids*, 7:L082601, 2022.
- [10] P. Cifani, M. Viviani, and K. Modin. An efficient geometric method for incompressible hydrodynamics on the sphere. *J. Comput. Phys.*, 473:111772, 2023.
- [11] David G. Dritschel, Wanming Qi, and J. B. Marston. On the late-time behavior of a bounded, inviscid two-dimensional flow. *J. Fluid Mech.*, 783:1–22, 2015.
- [12] D. Ebin and J. Marsden. Groups of diffeomorphisms and the motion of an incompressible fluid. *Ann. of Math. (2)*, 92:102–163, 1970.
- [13] S. Ephrati, P. Cifani, M. Viviani, and B. Geurts. Data-driven stochastic spectral modeling for coarsening of the two-dimensional euler equations on the sphere, 2023.
- [14] S. Ephrati, E. Jansson, A. Lang, and E. Luesink. An exponential map free implicit midpoint method for stochastic lie-poisson systems, 2024.
- [15] L. Euler. Principes généraux de l’état d’équilibre d’un fluide. *Académie Royale des Sciences et des Belles-Lettres de Berlin, Mémoires*, 11:217–273, 1757.
- [16] A. Franken, M. Caliaro, P. Cifani, and B. Geurts. Zeitlin truncation of a shallow water quasi-geostrophic model for planetary flow. *J. Adv. Model. Earth Sys.*, 16(6):e2023MS003901, 2024.
- [17] A. Franken, E. Luesink, S. Ephrati, and B. Geurts. Critical latitude in global quasi-geostrophic flow on a rotating sphere. *arXiv:2409.05432*, 2024.



- [18] A. Franken, E. Luesink, S. Ephrati, and B. Geurts. Casimir preserving numerical method for global multilayer geostrophic turbulence. *J. Comput. Phys.*, page 114155, 2025.
- [19] Ernst Hairer, Christian Lubich, and Gerhard Wanner. *Geometric Numerical Integration*, volume 31 of *Springer Series in Computational Mathematics*. Springer-Verlag, Berlin, second edition, 2006.
- [20] J. Hoppe. Diffeomorphism groups, quantization, and  $SU(\infty)$ . *Int. J. Modern Phys. A*, 04(19):5235–5248, 1989.
- [21] J. Hoppe and S.-T. Yau. Some properties of matrix harmonics on  $S^2$ . *Comm. Math. Phys.*, 195(1):67–77, 1998.
- [22] Robert H Kraichnan. Inertial ranges in two-dimensional turbulence. *The Physics of Fluids*, 10(7):1417–1423, 1967.
- [23] Y. Le Floch. *A brief introduction to Berezin-Toeplitz operators on compact Kähler manifolds*. Springer, 2018.
- [24] AnA.drew Majda and X. Wang. *Nonlinear Dynamics and Statistical Theories for Basic Geophysical Flows*. Cambridge University Press, 2006.
- [25] Robert I. McLachlan. Explicit Lie-Poisson integration and the Euler equations. *Phys. Rev. Lett.*, 71(19):3043–3046, 1993.
- [26] K. Modin and S. C. Preston. Zeitlin’s model for axisymmetric 3D Euler equations. *Nonlinearity*, 38(2):025008, 2025.
- [27] K. Modin and M. Roop. Spatio-temporal lie–poisson discretization for incompressible magnetohydrodynamics on the sphere. *IMA Journal of Numerical Analysis*, page draf024, 2025.
- [28] K. Modin and A. Suri. Geodesic interpretation of the global quasi-geostrophic equations, 2025.
- [29] K. Modin and M. Viviani. A Casimir preserving scheme for long-time simulation of spherical ideal hydrodynamics. *J. Fluid Mech.*, 884, 2020.
- [30] K. Modin and M. Viviani. Lie–poisson methods for isospectral flows. *Found. Comput. Math.*, 20(4):889–921, 2020.
- [31] K. Modin and M. Viviani. Canonical scale separation in 2d incompressible hydrodynamics. *J. Fluid Mech.*, 943:A36, 2022.
- [32] K. Modin and M. Viviani. Two-dimensional fluids via matrix hydrodynamics. arXiv:2405.14282, 2024.
- [33] L. Onsager. Statistical hydrodynamics. *Il Nuovo Cimento (1943-1954)*, 6(2):279–287, 1949.
- [34] Cecilia Pagliantini. Geometric low-rank approximation of the zeitlin model of incompressible fluids on the sphere, 2025.
- [35] M. Roop and S. Ephrati. Thermal quasi-geostrophic model on the sphere: derivation and structure-preserving simulation, 2025.
- [36] V. Zeitlin. Finite-mode analogs of 2D ideal hydrodynamics: coadjoint orbits and local canonical structure. *Phys. D*, 49(3):353–362, 1991.
- [37] V. Zeitlin. Self-consistent finite-mode approximations for the hydrodynamics of an incompressible fluid on nonrotating and rotating spheres. *Phys. Rev. Lett.*, 93:264501, 2004.
- [38] V. Zeitlin. On self-consistent finite-mode approximations in (quasi-) two-dimensional hydrodynamics and magnetohydrodynamics. *Phys. Lett. A*, 339(3-5):316–324, 2005.
- [39] V. Zeitlin. *Geophysical fluid dynamics: understanding (almost) everything with rotating shallow water models*. Oxford University Press, 2018.
- [40] Ge Zhong and Jerrold E. Marsden. Lie-Poisson Hamilton-Jacobi theory and Lie-Poisson integrators. *Phys. Lett. A*, 133(3):134–139, 1988.

Received xxxx 20xx; revised xxxx 20xx; early access xxxx 20xx.